Ocean & Sea Ice SAF

Associated & Visiting Scientist Activity Report

Triple Comparison of OSI SAF Low Resolution Sea ice drift products

Reference: CDOP-SG06-VS02

Version v1.3

28/09/2010

(Phil) Byongjun Hwang
Thomas Lavergne

Documentation Change Record

Version	Date	Author	Description
V0.0	27/05/10	PH	first draft
V0.1	10/09/10	TL	Comments by TL
V1.0	20/09/10	PH	Major re-writting by PH
V1.1	27/09/10	TL	Comments and small corrections
V1.2	27/09/10	PH	Minor corrections
V1.3	28/09/10	PH	Adopt minor comments by Anne O'Carrol

CONTENTS

1. Introduction

1.1 Overview

OSI SAF Low Resolution Sea Ice Drift (OSI-405) and Medium Resolution Sea Ice Drift (OSI-407) products were introduced as a result of the first Continuous Development and Operations Phase [CDOP, 2007 to 2012]. After sucessful development of these products under joint met.no and DMI responsibility (hereafter Project Team), the Operational Readiness Review (ORR) for OSI-405 (October 2009) concluded in the need for extending the validation exercise of these products in order to:

- conduct an inter-comparison with the products of IFREMER/Cersat (hereafter IFR),
- and gain confidence in the error statistics of the single-sensor OSI-405 datasets (from AMSR-E, ASCAT and SSM/I) as a step towards the multi-sensor OSI-405 dataset.

Both the cited ORR and an earlier Product Consolidation Review (PCR) suggested to setup a Associated & Visiting Scientist Activity (AVSA) for tackling some of the two aspects. A proposal for AVSA, submitted in Janaury 2010, has been approved mid-Februray 2010. In the proposal, two reports were identified - the first one focusing on inter-comparison with IFR products and the second one focusing on 3-way comparison of OSI-405 single sensor products. The first report, produced by AVSA on 27/05/10, containted the sensitivity study and validation results of both OSI SAF and IFR products.

This second report addresses the issue of 3-way comparison of OSI-405 single sensor products. We adapt triple-collocation methods (aka 3-ways uncertainty analysis) that has successfully been applied to Sea Surface Temperature (O'Carrol et al. 2008) and Surface Winds (Stoffelen 1998) but not, to our knowledge, to sea ice motion. At the kick-off meeting held on 11 March 2010 at met.no, both Project Team and VS agreed on 3-way error analysis of single-sensor OSI-405 (Low Resolution) products. In this report we also added ITP data into 3-way error analysis, i.e., two OSI-405 product and ITP data to see how 3-way error statistics change in different combination of datasets. This report contains the results and discussion of triple comparison of three OSI-405 products (AMSR, ASCAT, SSM/I) and ITP data. The report also provides statistics, graphs, and information about collocation procedure and software used.

1.2 Glossary

AMSR-E	Advanced Microwave Scanning Radiometer for EOS
ASAR	Advanced Synthetic Aperture Radar
ASCAT	Advanced SCATterometer
AVHRR	Advanced Very High Resolution Radiometer
CERSAT	Center for Satellite Exploitation and Research
CDOP	Continuous Development and Operations Phase
CMCC	Continuous Maximum Cross Correlation
DMI	Danish Meteorological Institute
DTU	Technical University of Denmark

GCTP	General Cartographic Transformation Package
GPS	Global Positioning System
IFREMER	French Research Institute for Exploitation of the Sea
ITP	Ice Tethered Profiler
NSIDC	National Snow and Ice Data Center
MCC	Maximum Cross Correlation
met.no	Norwegian Meteorological Institute
OSI SAF	Ocean and Sea Ice Satellite Application Facility
QuikSCAT	Quick SCATterometer onboard Seawinds satellite
SSM/I	Special Sensor Microwave/Imager

2. Sea ice drift products and ITP data

2.1 Sea ice drift products

In this report we targeted three OSI-405 single-sensor sea ice drift products for 3-way uncertainty analysis (Table 1). OSI-405 product datasets were obtained directly from Project Team at the AVSA kick-off meeting. The three OSI-405 (low resolution) ice drift are computed on a daily basis from aggregated maps of passive microwave (AMSR-E and SSM/I) or scatterometer (ASCAT) data (Table 1) [1]. The three products share similar spatial resolution and footprint size (Table 1).

Product	Instrument	Platform	Channels	Spatial Sampling (km)	Area averaging (km^2)
OSI-405 AMSR	AMSR-E	EOS Aqua	37 GHz, H+V pol.	62.5	~140x140
OSI-405 SSM/I	SSM/I	DMSP-F15	85 GHz, H+V pol.	62.5	~140x140
OSI-405 ASCAT	ASCAT	Metop-A	C band $\sigma°$	62.5	~140x140

Table 1: Sensor characteristics for the sea ice drift products used in this report.

Area averaging is the area covered by the sub-images used in computing the cross-correlation metric and, thus, the motion vector. Ice drift products indeed do not contain the motion vector of a single point but instead the average motion over a rather large area of sea ice. OSI-405 products adopt Continuous Maximum Cross Correlation (CMCC) method [1], where pixel values in the sub-images are interpolated from those in the nominal pixels. This is a more advanced method than the classical Maximum Cross Correlation (MCC) which is used in other sea ice products, e.g. Ifremer/Cersat and OSI-407 sea ice drift products [2-4]. The main advantage of CMCC method is in minimizing the quantification effects which is significant in low resolution products [4].

2.2 Ice Tethered Profiler data

The Ice Tethered Profilers (ITP) platforms are advanced autonomous drifting instruments that are designed to measure temperature and salinity profiles in the ocean under sea ice. As part of its daily data stream, each ITP transfers hourly unfiltered GPS locations. During the validation period, a total of 37 ITPs are available (both active and completed missions). The data density of ITPs are much less than Argos-based buoys, but it is benefited from much more accurate GPS location of the trajectories.

The Ice-Tethered Profiler data were collected and made available by the Ice-Tethered Profiler Program based at the Woods Hole Oceanographic Institution (http://www.whoi.edu/itp).

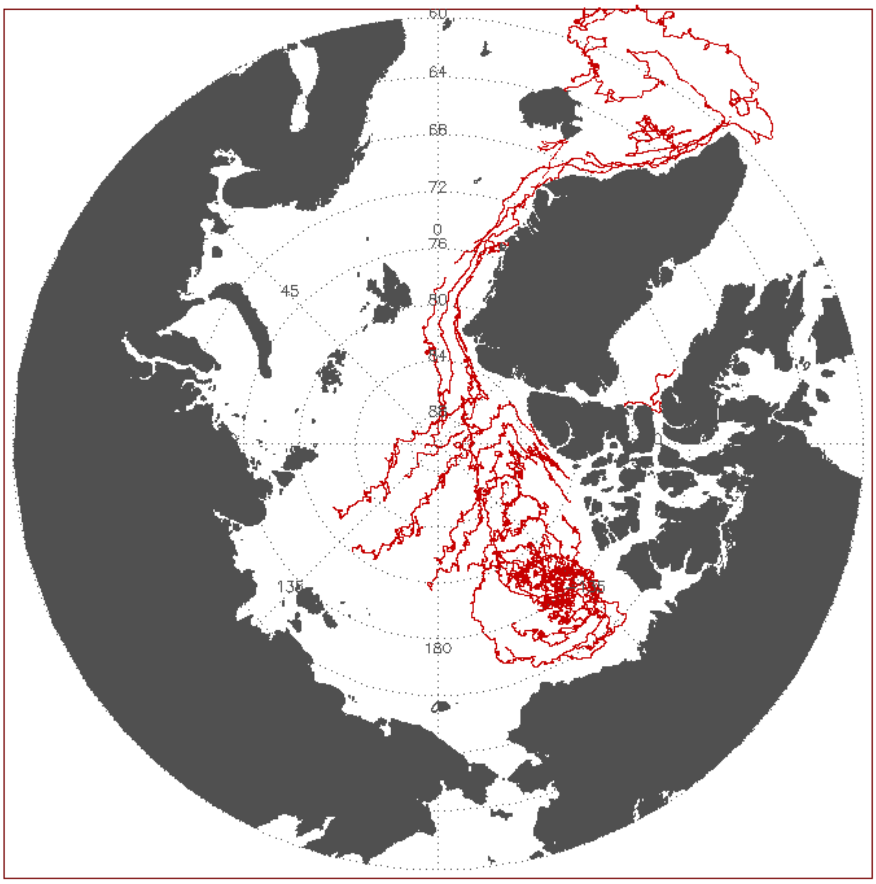

Figure 1: Map of ITP GPS trajectories.

3. Triple-collocation methodology

3.1 Variables and collocation details

The primary variables are the X and Y displacement components in the product grid, namely dX and dY. The selection of dX and dY is based on the fact that these variables tend to less biased than vector direction and magnitude [5].

Five experiments were designed to check the variability of error statistics (Table 2). Triple collocation data sets for experiments 1-4 were made for four different regions of the Arctic Ocean. The collocation criteria was that observation in a collocation triplet must be within [-3,+3] hours at the same product grid. Collocation data sets for experiments 5 were made for ITP locations, meaning that observation in sea ice drift products must be within [-1,+1] hour and 40 km from a ITP point [6] and then we selected only the triplets within [-3,+3] hours of each other at the same product grid. We used the 3-hour constraint to obtain more collocation triplets considering the swath time between three satellite sensors. All collocation was made during the period of 10/2008 to 05/2009.

Experiment	Collocation data	Collocation Region
1	AMSR, ASCAT, SSMI	Pan-Arctic (>70N)
2	AMSR, ASCAT, SSMI	Beaufort (>70N,180W-120W)
3	AMSR, ASCAT, SSMI	Eurasian (>70N, 30E-180E)
4	AMSR, ASCAT, SSMI	Fram Strait (>70, 30W-20E)
5	AMSR, ASCAT, SSMI	ITP location

Table 2: Details of experiments, collocation data, period and region.

3.2 Statistics

So called 3-way uncertainty analysis has been applied in Surface Winds [5] and Sea Surface Temperature [7]. The key concept of 3-way analysis is that 3 independent measurement methods sample a single “true value”. True value must be of some variables at time-space domain (e.g. sea surface temperature, x or y displacement of sea ice drift). The choice of the “true value” controls the interpretation of the statistics obtained through 3-way uncertainty analysis (see section 3.3). O'Carrol et al [7] argued that, if the errors in the three observation types are uncorrelated, then the variance of the error in three observation type 1, 2 and 3 can be expressed by

$$\sigma_1^2=\frac{1}{2}(V_{12}+V_{31}-V_{23}) \quad , \qquad \text{(Eq. 1a)}$$

$$\sigma_2^2=\frac{1}{2}(V_{23}+V_{12}-V_{31}) \quad \text{, and} \qquad \text{(Eq. 1b)}$$

$$\sigma_3^2=\frac{1}{2}(V_{31}+V_{23}-V_{12}) \quad . \qquad \text{(Eq. 1c)}$$

Here V_{ij} is the variance of the difference between observation type i and j.

3.3 Choice of true value and error budget

The method of 3-way uncertainty analysis aims at quantifying a random error (e.g. measurement error) around a “true value”. As argued by [7], such a quantification is not possible with only 2 sets of uncertain measurements. One often has to select one of the measurement methods as the “truth” (e.g. the buoy) and the other as uncertain (e.g. the satellite product). Under given hypotheses, access to 3 series of measurement allows to fully characterize the random noise around the “true value”.

In this report, we define the “true value” as the 48-hour displacement vectors of a 140x140 km^2 area of ice surface. The starting time varies from time to time depending on satellite overpass of the grid point (e.g. 10, 15 or 19 utc). The definition of this true value, results in identifying different error budgets for each sea ice drift measurement methods. For each ice drift observation method (three OSI-405 products), we identify 3 error sources:

- σ_T is the uncertainty due to temporal collocation;
- σ_S is the uncertainty due to spatial collocation;
- σ_O is the observation noise.

The temporal collocation error σ_T is negligible because we used the sensing time ([1, section 4.2.2]) as start time (t0) at each grid point and triple collocations were made with strict criteria (i.e. within 3 hours). The OSI-405 vectors are all processed on the same grid so that the uncertainty due to spatial collocation σ_S is zero. An observation error σ_O is identified which is the random error due to the ice tracking algorithm. Thus, considering our definition of the true value and the rather stringent collocation criteria we have used, the σ statistics reported in the following sections mainly correspond to σ_O for OSI-405 products.

4. Results and Discussions

4.1 Triple error analysis of three OSI-405 products

Triple error statistics of three OSI-405 products, resulting from applying Eq 1a to 1c, are listed in Table 3. It is striking to see the AMSR σ values are quite different between Experiments, i.e. the AMSR σ is as small as 1.90 km at Experiment 2 and up to 5.23 km at Exp 3 (Table 3). In fact this is rather puzzling to see AMSR σ values are sometimes larger than SSMI ones or even than ASCAT ones (in Exp 3). It was indeed found that AMSR has shown the smallest errors against drifting GPS buoys in the validation study by the Project Team [8], so it is expected to see smaller σ values of AMSR than the ones of the other two products.

Experiment	N	AMSR (dX,dY) (km)	ASCAT (dX, dY) (km)	SSMI (dX, dY) (km)
1 (Pan-Arctic)	12798	3.78, 3.83	4.31, 4.77	3.29, 3.40
2 (Beaufort)	5395	1.90, 2.17	3.74, 3.96	3.02, 2.93
3 (Eurasian)	5189	5.28, 4.92	4.68, 4.85	3.57, 3.31
4 (Fram)	286	2.05, 3.90	6.35, 7.03	3.47, 6.35
5 (ITP)	90	2.29, 2.60	4.74, 3.92	3.27, 2.73

Table 3: The triplet σ values and number of collocation triplets N of three OSI-405 products for each experiments.

The results can divide into two contrasting groups, A) Pan-Arctic/Eurasian and B) Beaufort/Fram/ITP. In the group A, SSMI always has the smallest s values, while ASCAT the largest in Pan-Arctic case and AMSR the largest in Eurasian sector. In the group B, AMSR always shows the smallest σ values, followed by SSMI and ASCAT. This contrasting results can be explained by their regional distributions. Considering ITP data (major source of drifting trajectories) are mainly concentrated in Beaufort Sea and Fram Strait regions (Fig. 1), it is not surprising to see the triplet σ values from those regions share as the same trend as seen in the validation study against drifting buoys, i.e. AMSR<SSMI<ASCAT. In the validation study against drifting buoys [8], the uncertainty of AMSR, SSMI and ASCAT were 2.56/2.59 km, 3.95/3.83 km, and 4.35/4.19 km, respectively. Note that the triplet σ values are always smaller than those values in [8] except ASCAT at Exp. 4. This is probably true because the triplet σ is a measure of error around "true value". However the error against drift GPS trajectories contains other errors: the errors due to GPS positiong and the errors due to sampling ice motion at different scales (i.e. a point trajectories of buoy vs. area average of drift product). It cannot, however, explain why ASCAT σ values at Exp 4 are so high.

While it is comforting that triplet σ values in the group B are similar to what we expected from previous validation study, it is still puzzling why such high AMSR σ values occur in Pan-Arctic scale and especially Eurasian sector of the Arctic. It is likely that the error statistics in Eurasian sector increase the triplet errors of AMSR in the Pan-Arctic scale, while the error statistics in Beaufort Sea and Fram Strait affect in an opposite way. Sea ice regime between Eurasian sector and Beaufort/Fram regions is contrasting. Eurasian sector is mostly a seasonal ice zone where first-year ice is the dominant ice type especially after 2008, while good fraction of multiyear ice occur in Beaufort Sea and Fram strait [9]. Is then this different sea ice regime related to contrasting triplet σ values? No robust conclusions can be drawn in this report. However, those preliminary results are still interesting as they challenge the generalization of statistical results obtained over areas where multi-year ice conditions prevail (ITP locations) to other regions of the Arctic or at Pan-arctic scale.

4.2 Seasonal variability

For further examination of contrasting triplet σ values between regions, we analyze the seasonal variability of σ for three ice drift products for Beaufort Sea (Exp 2) and Eurasian Sector (Exp 3) (Fig. 2). In Beaufort Sea the AMSR σ values are consistently smaller than the others. Note that AMSR values become more smaller during October while ASCAT and SSMI values are much larger (Fig. 2). October in Beaufort Sea can be characterized as freeze-up, i.e. forming new ice or refreeze of old ice. The physical characteristics of sea ice become highly variable in spatial and temporal scale, e.g. bare new ice is quickly covered with frost flowers followed by snow [10] and this period is also characterized by higher cloud fraction [11]. It is observed that C-band backscattering values (ASCAT) are very sensitive to frost flowers, snow depth and pancake ice [12], while passive microwave brightness temperatures at 85 GHz (SSMI) are significantly affected by atmosphere [13]. These factors may contribute higher σ values in ASCAT and SSMI. On the other hands, brightness temperatures at 37 GHz (i.e. AMSR) are less affected by atmosphere and become stable once it is snow or frost flower covered [10]. This may contribute smaller σ values in AMSR. In Eurasian sector AMSR s values become much larger during December and January and continuously higher or comparable to ASCAT values during February to April (Fig. 2). While no solid explanation for this can be found with current datasets and analysis, it appears SSMI (85 GHz) tracks the ice drift better in first-year dominant region.

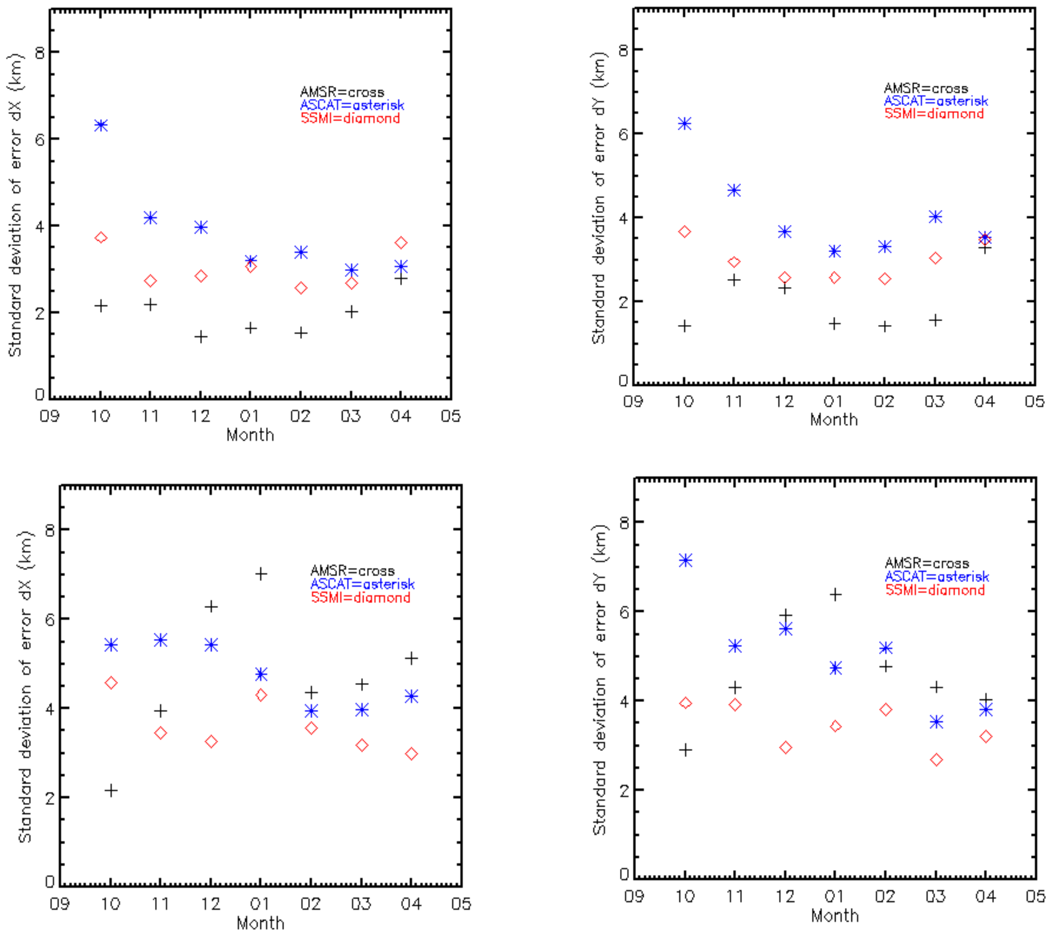

Figure 2: Seasonal variability of triplet s values in Beaufort Sea (experiment 2, top row) and Eurasian sector (experiment 3, bottom row).

5. Summary and Conclusions

3-way uncertainty analysis has been conducted for OSI-SAF Low Resolution (405, AMSRE, SSM/I (F15) and ASCAT) sea ice drift products. Triple collocations were made for 5 experiments of various combination of the different regions of the Arctic; Pan-Arctic, Beaufort Sea, Eurasian sector, Fram Strait and ITP location. We selected rather strict collocation criteria to make triplets, i.e. the start time (t0) of the products should be within [-3,+3] hours each other, so that the triplet errors (σ) represent random observational errors around "true value" due to tracking algorithm and base map.

Triplet σ values of three OSI-405 products have shown very contrasting divisions between regions. For the regions of Beaufort Sea, Fram Strait and ITP location the AMSR σ values were the smallest, followed by SSMI and ASCAT. This was the expected trend from the previous validation study against drifting buoys [8]. The σ values from triplets were slightly smaller than the ones found in [8], and this might be attributed to different validation period and methods and/or simply due to the fact that the triplet σ is a measure of error around "true value", but the error against drift GPS trajectories contains other errors e.g. GPS errors and errors due to tracking ice motion at different scales (representativity error). While it iss comforting to see that the triplet σ values show a trend similar to the validation study [8] in those regions, it was puzzling however to see the triplet σ values had the opposite trend in other regions. Indeed, for Pan-Arctic and Eurasian sector, SSMI had the smallest σ values. Analysis of the seasonal variability of the triplet σ values shows some interesting features, but that were not sufficient to robustly explain the contrasting features mentioned above.

Although no robust conclusions can be drown from this short research project, we think it is likely the contrasting sea ice regimes between the two groups of regions, i.e. multiyear ice dominant (Beaufort/Fram/ITP) vs. first-year ice dominant (Eurasian) that might be related to the contrasting triplet σ values. Indeed, although the same sea ice motion tracking algorithm (CMCC) is applied everywhere, the various imaging technologies (active vs passive) and wavelengths react differently to the presence of multiyear ice. Furthermore, those preliminary results are interested per se as they challenge the generalization of validation statistics obtained in some regions of the Arctic, at ITP locations (see Figure 1) to the pan-Arctic scale. Some answers of the question might be found from more validation study, e.g. in designing n-way (four or five or so) error analysis including ASAR ice drift and in make use of ice type products (multi vs first year ice) in future updates of the OSI-405 validation report ([8]).

6. References

[1] Lavergne, T. and S. Eastwood (2010, March). Low resolution sea ice drift Product User's Manual – v1.4. Technical Report SAF/OSI/CDOP/met.no/TEC/MA/128, EUMETSAT OSI SAF – Ocean and Sea Ice Satellite Application Facility.

[2] Girard-Ardhuin, F., R. Ezraty, D. Croizé-Fillon, and J.-F Piollé (2008, April). Sea Ice Drift in The Central Arctic Combining QuikSCAT and SSM/I Sea Ice Drift Data – User's Manual v3.0, CERSAT, IFREMER, France.

[3] Dybkjaer, G. (2009, July). Medium Resolution Sea Ice Drift Proudct User Manual - v1.0, EUMETSAT OSI SAF - Ocean and Sea Ice Satellite Application Facility.

[4] Ezraty, R., F. Girard-Ardhuin, and J.-F.Piollé (2007, February). Sea Ice Drift in The Central Arctic Estimated From SEAWINDS/QuikSCAT Backscatter Maps – v2.2, CERSAT, IFREMER, France.

[5] Stoffelen, A. (1998). Toward the true near-surface wind speed: Error modeling and calibration using triple collocation. J. Geophys. Res. 103(C4), 7755-7766.

[6] Hwang, B.J., and T. Lavergne (2010 Sept). Validation and Comparison of OSI SAF Low and Medium Resolution and IFREMER/Cersat Sea ice drift products, EUMETSAT Associated & Visiting Scientist Activity Report, SAF/OSI/CDOP/met.no/SCI/RP/151, EUMETSAT OSI SAF – Ocean and Sea Ice Satellite Application Facility.

[7] O'Carrol, A. G., J. R. Eyre, and R. W. Saunders, (2008). Three-way error analysis between AATSR, AMSR-E and in situ sea surface temperature observations, Journal of Atmospheric and Oceanic Technology, pp. 1197-1207, doi:10.1175/2007JTECHO542.1.

[8] Lavergne, T., Eastwood, S., Teffah, Z., Schyberg, H., and Breivik, L.-A.. Sea ice motion from low resolution satellite sensors: an alternative method and its validation in the Arctic. *J. Geophys. Res.*, doi:10.1029/2009JC005958, *in press*, 2010.

[9] Kwok, R., G.F. Cunningham, M. Wensnahan, I. Rigor, H.J. Zwally, and D. Yi (2009), Thinning and volume loss of the Arctic Ocean sea ice cover: 2003-2008, *J. Geophys. Res.*, 114, C07005, doi:10.1029/2009JC005312.

[10] Hwang, B.J., J.K. Ehn, D.G. Barber, R. Galley, and T.C. Grenfell (2007) Investigations of newly formed sea ice in the Cape Bathurst polynya: 2. Microwave emission. J. Geophys. Res. 112(C05003), doi: 10.1029/2006JC003703.

[11] Wang, X, and J.R. Key (2005) Arctic Surface, Cloud, and Radiation Properties Based on the AVHRR Polar Pathfinder Dataset. Part 1: Spatial and Temporal Characteristics, *J. Clim.* 18, 2558-2574.

[12] Isleifson, D., B.J. Hwang, D.G. Barber, R. Scharien, and L. Shafai, (2010) C-Band Polarimetric Backscattering Signatures of Newly Formed Sea Ice during Fall Freeze-up, IEEE Trans. Geo. Rem. Sens.

[13] Mätlzer, C. (1992), Ground-based observations of atmospheric radiation at 5, 10, 21, 35, and 94 GHz, *Radio Sci.*, 3646-3658.

APPENDIX A: Collection software

IDL v7.0.0 (© 2007 ITT Visual Information Solutions) was used throughout all the collocation procedure and plotting the graphs (http://www.ittvis.com/). IDL sub-routines were coded by the VS to read directly from raw data format of each product and ITP data. The main IDL code reads the all necessary sub-routines required.

3-way collocations were conducted by using IDL codes;

- tri_col_405_asmr_ssmi_asct.pro: makes triple collocation of AMSR, SSMI and ASCAT proudcts,
- tri_col_405_itp_amsr_ascat.pro: makes triple collocation of ITP, AMSR and ASCAT products,
- tri_col_405_itp_amsr_ssmi.pro: makes triple collocation of ITP, AMSR and SSMI products,
- tri_col_405_itp_ssmi_ascat.pro: make triple collocation of ITP, SSMI, ASCAT products.

The three OSI-405 products share the same product grid and triple collocation was made by extracting the dX and dY at the same grid point.

In order to obtain triple collocation data set including ITP data, I first run the IDL codes;

- colloc_os405_ascat_w_itp_all_wi_100km_3hr_final2.pro,
- colloc_os405_asmr_w_itp_all_wi_100km_3hr_final2.pro,
- colloc_os405_ssmif5_w_itp_all_wi_100km_3hr_final2.pro.

These IDL code makes collocation data set that grips all ITP points within 100 km radius from each product grid, and then only one nearest ITP point is selected by using code;

- find_nearest_tri_col.pro.

Calculating the error statistics and plotting graphs are all done by the codes;

- tri_col_statistics_amsr_ssmi_ascat.pro,
- tri_col_statistics_amsr_asct_itp.pro,
- tri_col_statistics_amsr_ssmi_itp.pro,
- tri_col_statistics_ssmi_ascat_itp.pro.

Map projection utility:

Note all the calculation was made using GCTP Projection package embedded in IDL 7.0.0.

List of IDL **sub-routines:**

- read_itpdata_file.pro: read single ITP data file
- get_all_itpdata_files.pro: load all ITP info (outputs: ref_JD, ref_lon, ref_lat, ref_ln)
- get_osi_saf_405_amsre.pro
- get_osi_saf_405_ascat.pro

- get_osi_saf_405_ssmi_f15.pro
- read_final_amsr_itp.pro
- read_final_ascat_itp.pro
- read_final_ssmi5_itp.pro